Insights into nuclear saturation density from parity-violating electron scattering

C. J. Horowitz [1,*] J. Piekarewicz [2,†] and Brendan Reed [1,3,‡]

[1]*Center for the Exploration of Energy and Matter and Department of Physics, Indiana University, Bloomington, Indiana 47405, USA*

[2]*Department of Physics, Florida State University, Tallahassee, Florida 32306, USA*

[3]*Department of Astronomy, Indiana University, Bloomington, Indiana 47405, USA*

(Received 14 July 2020; accepted 28 September 2020; published 19 October 2020)

The saturation density of nuclear matter ρ_0 is a fundamental nuclear physics property that is difficult to predict from fundamental principles. The saturation density is closely related to the interior density of a heavy nucleus, such as ^{208}Pb. Parity-violating electron scattering can determine the average interior weak charge and baryon densities in ^{208}Pb. This requires not only measuring the weak radius $R_{\rm wk}$ but also determining the surface thickness of the weak charge density a. We use the PREX experimental result for the weak radius of Pb and assume a 10% theoretical uncertainty in the presently unmeasured surface thickness to obtain $\rho_0 = 0.150 \pm 0.010$ fm^{-3}. Here the 7% error also has contributions from the extrapolation to infinite nuclear matter. These errors can be improved with the upcoming PREX II results and with a new parity-violating electron scattering experiment, at a somewhat higher momentum transfer, to determine a.

DOI: 10.1103/PhysRevC.102.044321

I. INTRODUCTION

The saturation density of nuclear matter ρ_0 is very important for the structure of nuclei. Infinite nuclear matter, a hypothetical uniform system of protons and neutrons without Coulomb interactions, is expected to have an energy per nucleon that is minimized at ρ_0. This minimum describes nuclear saturation and is a fundamental nuclear-structure property. Furthermore, this value of ρ_0 is an important benchmark that is used to measure even higher density matter in astrophysics and in the laboratory. Nuclear saturation implies that the interior density of heavy nuclei should be nearly constant and close to ρ_0. Historically, the semiempirical mass formula [1,2] and the liquid drop model [3] describe the nucleus as an incompressible quantum drop at ρ_0. But why does nuclear matter saturate? And how can one calculate the saturation density ρ_0? Surprisingly, the answers to these deceptively simple questions have proved to be both subtle and elusive.

Liquid water saturates at a density of 1 g/cm^3 because of the size of the water molecules. Does nuclear matter saturate because of the finite nucleon size and, if so, does this size explain the value of $\rho_0 \approx 0.15$ fm^{-3}? The situation is likely more complicated. Nucleons are known to have repulsive cores because phase shifts for nucleon-nucleon scattering become negative at high energies. However, the core size is too small to explain the value of ρ_0 [4]. Indeed, nuclear matter calculations with only two-nucleon interactions may saturate at up to twice the expected density [5]. It is now believed that three- and higher-nucleon interactions are important for nuclear saturation and for determining ρ_0.

Chiral effective field theory (CEFT) provides a systematic expansion of the strong interaction between nucleons in powers of the momentum transfer over a suitable chiral scale [6–8]. This allows one to calculate the energy of nuclear matter to a given order in a chiral expansion. Note that CEFT includes two-, three-, and many-nucleon interactions. Under this framework, the empirical saturation point (density and energy per nucleon) are well reproduced within statistical and systematic uncertainties [9,10]. The uncertainty band comes from the truncation of the chiral expansion and from imposing a cutoff at high-momentum transfers. Whereas CEFT appears consistent with nuclear saturation at ρ_0, the error band in present calculations is too broad to make a sharp prediction of the actual value of ρ_0.

So if one cannot accurately compute ρ_0 from first-principle calculations, can one observe it? Strictly speaking, nuclear matter is an infinite system without Coulomb interactions, so observations of ρ_0 must involve an extrapolation from measurements in finite nuclei; see, for example, Ref. [11]. Nevertheless, the interior baryon density of heavy nuclei is expected to be fairly constant and close to ρ_0. Among heavy nuclei, ^{208}Pb may be particularly important because it is the heaviest stable doubly magic nucleus. As such, *the interior baryon density of* ^{208}Pb *may provide the finite nucleus observable that is most closely related to* ρ_0. In this paper we present a new measurement of the interior baryon density of ^{208}Pb based on results from the PREX experiment [12,13].

Unfortunately, we do not have detailed knowledge of the neutron density in ^{208}Pb; see Ref. [14] and references contained therein. The charge density is well measured so the proton density is accurately known [15]. However, ^{208}Pb has 44 excess neutrons, so the neutron density can be signifi-

*horowit@indiana.edu
†jpiekarewicz@fsu.edu
‡reedbr@iu.edu

 ©2020 American Physical Society

cantly different from the proton density. Given this incomplete information, our present best estimate of ρ_0 comes from a variety of empirical nuclear energy-density functionals. These functionals are calibrated to the binding energies and charge radii of a variety of nuclei and can then be used to predict ρ_0, see, for example, Refs. [16,17]. In particular, Reinhard and Nazarewicz argue that fitting charge radii sharply constrains ρ_0 [18].

Alternatively, if one can cleanly measure the interior neutron density of ^{208}Pb, then one should be able to infer ρ_0 with small and quantifiable uncertainties. Often neutron densities are determined with strongly interacting probes [19], such as antiprotons [20,21], elastic proton scattering [22], heavy-ion collisions [23], elastic pion scattering [24], and coherent pion photo production [25]. One typically measures cross sections or spin observables that involve the convolution of the neutron density with an effective strong-interaction range for the probe. Although these observables can be measured with small statistical uncertainties, complexities arising from the strong interaction introduce significant systematic errors in the extracted neutron densities [14].

It is also possible to measure neutron densities, or equivalently weak charge densities, with electroweak probes using coherent neutrino-nucleus scattering [26–29] or parity-violating (PV) electron scattering [12,30]. This is because the weak charge of a neutron is much larger than that of a proton, so the weak charge density of a nucleus is very closely related to its neutron distribution. Compared to strongly interacting probes, parity violation offers a clean and model-independent way to determine the weak charge density with much smaller uncertainties (statistical+systematic) than with strongly interacting probes. In the past few decades significant theoretical [30–37] and experimental [12,38] efforts have been devoted to improve parity-violating electron scattering experiments. At Jefferson laboratory, the radius of the weak charge density of ^{208}Pb was measured in the original PREX campaign [12,13] and is now being measured with increased precision during the follow-up PREX-II campaign [39]. At the same time, CREX will provide the first electroweak determination of the weak radius of ^{48}Ca [40].

Present parity-violating experiments focus on determining the rms radius of the weak charge density $R_{\rm wk}$ from a single measurement at a relatively low-momentum transfer. Yet additional features of the weak charge density $\rho_{\rm wk}(r)$ can be revealed by measuring the parity-violating asymmetry A_{pv} at higher-momentum transfers. If A_{pv} is measured at several momentum transfers, then a complete model independent representation of the weak charge density can be determined [41], either as Fourier Bessel expansion or as a sum of Gaussians. This is feasible for ^{48}Ca and may require measurements at six or seven momentum transfers. For ^{208}Pb, however, this is more challenging because a determination of $\rho_{\rm wk}$ in the nuclear interior requires a measurement at high-momentum transfer where the elastic cross section is very small.

What is then required to determine the saturation density ρ_0? In principle, one could follow these four steps: (a) Determine the entire weak charge density $\rho_{\rm wk}(r)$ of ^{208}Pb, (b) average over $\rho_{\rm wk}(r)$ in the interior to obtain a measure of the average weak charge density, (c) combine this average weak charge density with an average of the experimental charge density to obtain a measure of the interior baryon density, and (d) extrapolate such a value to the very closely related saturation density of infinite nuclear matter. Here we combine the first two steps in a manner that dramatically minimizes the need for parity-violating experiments.

II. FORMALISM

We propose, rather than to determine the full density, a simple representation of $\rho_{\rm wk}(r)$ using a symmetrized two-parameter Fermi function that is then used to perform the interior average. That is, we model $\rho_{\rm wk}(r)$ as [42,43]

$$\rho_{\rm wk}(r,c,a)=\rho^0_{\rm wk}\frac{\sinh(c/a)}{\cosh(r/a)+\cosh(c/a)}, \tag{1}$$

where c is the half-density radius, a the surface diffuseness, and the normalization constant is

$$\rho^0_{\rm wk}=\frac{3Q_{\rm wk}}{4\pi c(c^2+\pi^2a^2)}\Rightarrow\int d^3r\rho_{\rm wk}(r,c,a)=Q_{\rm wk}. \tag{2}$$

Here the total weak charge of a nucleus with N neutrons and Z protons is $Q_{\rm wk}=Q_nN+Q_pZ$, where (including radiative corrections [44,45]) $Q_n=-0.9878$ is the weak charge of a neutron, and $Q_p=0.0721$ that of a proton. For ^{208}Pb, $Q_{\rm wk}=-118.551$.

While the symmetrized Fermi (SFermi) function is practically indistinguishable from the conventional Fermi function, its superior analytic properties allows one to determine the form factor as well as all its moments in closed form [42,43]. In particular, the mean-square weak radius is

$$R^2_{\rm wk}=\frac{1}{Q_{\rm wk}}\int r^2\rho_{\rm wk}(r)d^3r=\frac{3}{5}c^2+\frac{7}{5}(\pi a)^2. \tag{3}$$

We propose to use $\rho^0_{\rm wk}$ in Eq. (2) as the measure of the average interior weak charge density, which for clarity we rewrite in terms of the weak radius $R_{\rm wk}$ rather than c:

$$\rho^0_{\rm wk}=\frac{27Q_{\rm wk}}{4\pi\left(5R^2_{\rm wk}-4\pi^2a^2\right)\sqrt{15R^2_{\rm wk}-21\pi^2a^2}}. \tag{4}$$

Given that we are interested only in the average density $\rho^0_{\rm wk}$ rather than on the full density, PV experiments need only to determine the weak radius $R_{\rm wk}$ and the surface thickness a. The existing PREX and PREX II [39] measurements are primarily sensitive to $R_{\rm wk}$, so an additional PV experiment at a somewhat higher-momentum transfer could determine a [43]. We will describe this experiment in a forthcoming paper.

We illustrate our procedure in Fig. 1, which shows the experimental charge density of ^{208}Pb along with a SFermi function fit that yields: $c_{\rm ch}=6.6658$ fm, $a_{\rm ch}=0.51219$ fm, and a corresponding charge radius of $R_{\rm ch}=5.5031$ fm [15]. In turn, this implies a normalization of $\rho^0_{\rm ch}=0.06246$ fm^{-3}. This is our measure of the average interior charge density of ^{208}Pb. Figure 1 also shows a model weak charge density as predicted by the FSUGold relativistic mean-field interaction [46] and the corresponding SFermi function fit. The SFermi functions—which average over shell oscillations—are seen to be very good representations of both the (electromagnetic) charge and weak charge densities. Note that we are

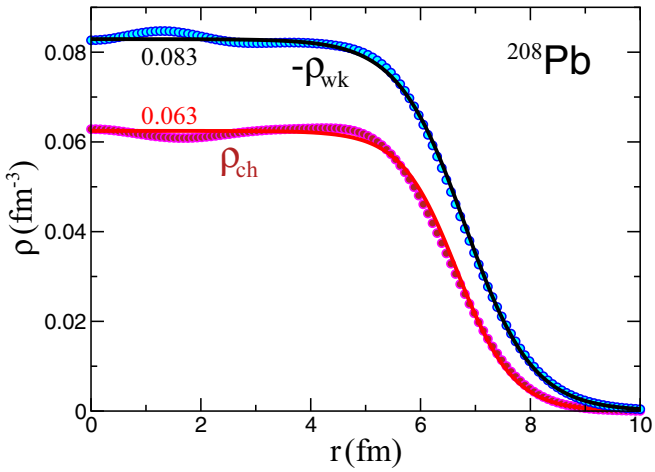

FIG. 1. The experimental charge density of ^{208}Pb [15] (red circles) and the corresponding SFermi function fit (solid red line). Also shown is the weak charge density as predicted by the FSUGold interaction [46] (blue circles) along with a SFermi function fit (solid black line).

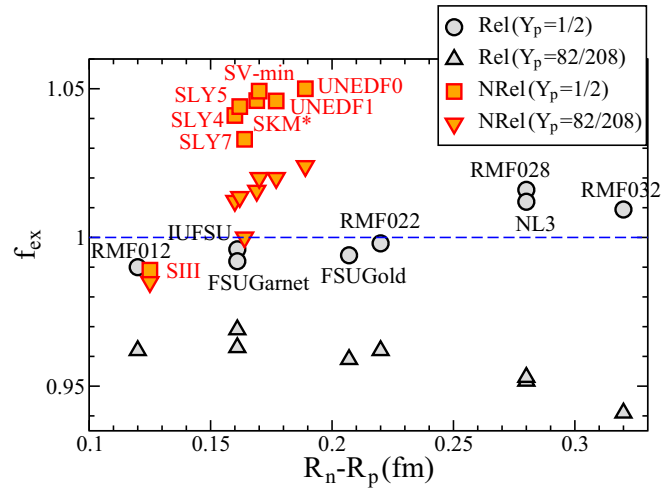

FIG. 2. The extrapolation factor f_{ex} defined in Eq. (6) as a function of the the neutron skin thickness of ^{208}Pb for a number of nonrelativistic and relativistic EDFs. Shown with triangles is the extrapolation factor $\widetilde{f}_{ex}$ to asymmetric nuclear matter with the same ratio of neutrons to protons as ^{208}Pb.

not proposing to use model predictions for the weak charge density but rather a SFermi function with both parameters R_{wk} and a determined from experiment.

We now combine the average interior weak and charge densities to obtain an estimate of the average interior baryon density ρ_b^0. That is,

$$\begin{aligned}\rho_b^0 &= \rho_n^0 + \rho_p^0 = \frac{1}{Q_n}\left(\rho_{wk}^0 - Q_p\rho_{ch}^0\right) + \rho_{ch}^0 \\ &= \frac{1}{Q_n}\rho_{wk}^0 + \left(1 - \frac{Q_p}{Q_n}\right)\rho_{ch}^0 \\ &= -(1.0123)\rho_{wk}^0 + (1.0730)\rho_{ch}^0. \end{aligned} \tag{5}$$

The final step is to extrapolate the interior baryon density ρ_b^0 to the closely related saturation density of infinite nuclear matter ρ_0. *We define an extrapolation factor* f_{ex} *as the saturation density of infinite nuclear matter* ρ_0 *over the average interior density of* ^{208}Pb:

$$f_{ex} = \frac{\rho_0}{\rho_b^0}. \tag{6}$$

We expect $f_{ex} \approx 1$. We estimate f_{ex} by considering a variety of relativistic and nonrelativistic energy-density functionals (EDFs). For each EDF one calculates point proton $\rho_p(r)$ and neutron $\rho_n(r)$ densities and then computes the weak density by folding these point-nucleon densities with a dipole nucleon form factor of radius $r_p = 0.84$ fm that accounts for the finite nucleon size. Next, one fits SFermi functions to the model weak and charge densities to obtain ρ_{wk}^0, ρ_{ch}^0, and ultimately ρ_b^0 from Eq. (5). Comparing this value of ρ_b^0 to the prediction for the saturation density ρ_0 yields f_{ex} for that particular EDF.

Results are plotted in Fig. 2 for the following nonrelativistic Skyrme functionals: SIII [47], SLY4, SLY5, SLY7, and SKM* [48], SV-min [17], UNEDF0 [49], and UNEDF1 [50]. We also include results for the following relativistic functionals: FSUGold [46], IUFSU [51], NL3 [52], FSUGarnet, RMF012, 022, 028, and 032 [53]. We see that f_{ex} is indeed close to one for all of the models that have been considered. However, if one looks in more detail, then f_{ex} for relativistic models is in general very close to one with a slight increase with increasing neutron skin (neutron minus proton radius $R_n - R_p$). This is likely related to the density dependence of the symmetry energy which increases with increasing neutron skin. Most of the nonrelativistic models that we consider predict $f_{ex} \approx 1.04$ and this is noticeably larger than for the relativistic functionals. This is an interesting result that may be related to the assumed density dependence of the various EDFs. For example, the old Skyrme force SIII, with $\gamma = 1$ for the density-dependent term $t_3\rho^\gamma$, predicts $f_{ex} \approx 0.99$ that is close to the prediction of most relativistic models. In contrast, all other Skyrme forces (shown in Fig. 2) have smaller values for γ and yield significantly larger f_{ex}.

The extrapolation from ρ_b^0 in ^{208}Pb to ρ_0 involves three effects. First, surface tension—which is absent in an infinite system—increases the density of lead and tends to make $f_{ex} < 1$. Second, Coulomb interactions which are ignored in infinite nuclear matter reduce the density of lead making $f_{ex} > 1$. To some extent, effects from surface tension and Coulomb interaction cancel out restoring $f_{ex} \approx 1$. Finally, one is extrapolating in isospin from the neutron rich lead nucleus to symmetric nuclear matter, as ρ_0 is the saturation density of symmetric nuclear matter.

To explore the consequences of the extrapolation in isospin, we define $\widetilde{\rho}_0$ as the saturation density of asymmetric nuclear matter with a proton fraction identical to that of ^{208}Pb, namely, $Y_p = 82/208 \simeq 0.39$. It is a simple matter to calculate $\widetilde{\rho}_0$ for all EDFs included in Fig. 2. Note that to a very good approximation $\widetilde{\rho}_0$ is given by [54]

$$\frac{\widetilde{\rho}_0}{\rho_0} = 1 - 3\frac{L}{K}\alpha^2 + \mathcal{O}(\alpha^4), \quad (\alpha = 1 - 2Y_p), \tag{7}$$

where K is the incompressibility coefficient of symmetric matter and L the slope of the symmetry energy. Following Eq. (6) we define in analogy $\widetilde{f}_{\rm ex} = \widetilde{\rho}_0/\rho_b^0$. Values for $\widetilde{f}_{\rm ex}$ are shown in Fig. 2 using up- and down-triangles. For relativistic functionals, $f_{\rm ex} \approx 1$ and the interior density of lead is close to the saturation density of symmetric nuclear matter. However, $\widetilde{f}_{\rm ex} < 1$ as $\widetilde{\rho}_0$ decreases with increases L, a quantity that is strongly correlated to $R_n - R_p$. In contrast, for nonrelativistic functionals $\widetilde{f}_{\rm ex} \approx 1$ so the interior density of lead is close to the saturation density of asymmetric nuclear matter.

This interesting difference between relativistic and nonrelativistic functionals should be explored using other models. For example, by building on ^{48}Ca [55,56], microscopic coupled cluster calculations for ^{208}Pb may become feasible in the near future. This could provide a microscopic determination of $f_{\rm ex}$ that is more closely connected to chiral two- and three-nucleon forces. Until then, we use all models in Fig. 2 to infer the following limit:

$$f_{\rm ex} \approx 1.02 \pm 0.03. \tag{8}$$

That is, the extrapolation to infinite nuclear matter introduces a $\sim$3% uncertainty in the inferred value of ρ_0.

In summary, PV experiments can determine both the radius $R_{\rm wk}$ and surface thickness a of the weak charge density of ^{208}Pb, from which the average weak density $\rho^0_{\rm wk}$ is calculated using Eq. (4). The known charge density $\rho^0_{\rm ch}$ is then added to $\rho^0_{\rm wk}$ in Eq. (5) to obtain ρ^0_b. This, in turn, is extrapolated to ρ_0 using Eqs. (6) and (8).

III. RESULTS

We present a first estimate of ρ_0 based on the existing PREX result of $R_{\rm wk} = 5.826 \pm 0.181$ fm [13]. Unfortunately, at present there is no electroweak experiment that constrains the surface thickness a. Thus, we provide a conservative theoretical estimate for a. Considering all EDFs in Fig. 2 yields a surface thickness in the 0.58 fm (SIII) to 0.632 fm (RMF032) range. We arbitrarily select the UNEDF0 result to define the central value and assign a very conservative 10% error that more than covers the theoretical range; that is, $a = 0.616 \pm 0.062$ fm. A future PV experiment at a slightly larger-momentum transfer to constrain a would allow a direct experimental determination of the interior weak density.

Adopting the PREX value for $R_{\rm wk}$, our theoretical assumption for a, and Eqs. (4) and (5) yields,

$$\rho^0_b = 0.1473 \pm 0.0084 \pm 0.0030 \ {\rm fm}^{-3}, \tag{9}$$

where the first error is from the PREX error in $R_{\rm wk}$ while the second error corresponds to our assumed 10% uncertainty in a. The last step is to multiply this result by $f_{\rm ex} = 1.02 \pm 0.03$ to get our present estimate for the saturation density of nuclear matter:

$$\rho_0 = 0.1502 \pm 0.0086 \pm 0.0031 \pm 0.0045 \ {\rm fm}^{-3}, \tag{10}$$

where the last error is due to the uncertainty in $f_{\rm ex}$. Adding all three errors in quadrature gives a total uncertainty of 7% that is dominated by the error in $R_{\rm wk}$. That is,

$$\rho_0 = 0.150 \pm 0.010 \ {\rm fm}^{-3}. \tag{11}$$

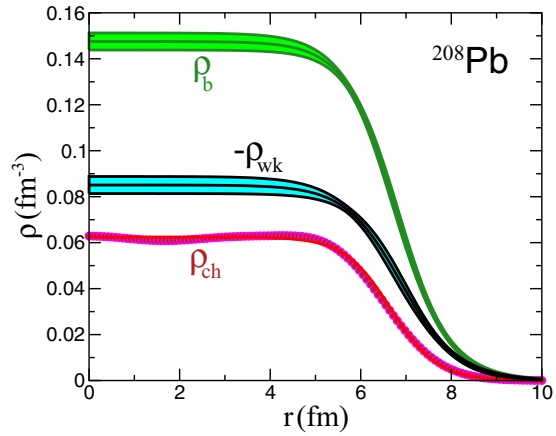

FIG. 3. Theoretical prediction for the baryon density of ^{208}Pb. The error band assumes that $R_{\rm wk}$ is measured to 1% and the surface thickness is constrained to 10%, see text for details. The corresponding curve for the weak charge density is also shown. Finally, the experimental charge density [15] is displayed along with a SFermi fit.

Our result is consistent, although somewhat lower, than the phenomenological estimate of $\rho_0 = 0.164 \pm 0.007$ fm^{-3} claimed in Ref. [9] based on some selected density functionals—yet fully consistent with $\rho_0 = 0.151 \pm 0.001$ fm^{-3} predicted by a relativistic EDF calibrated using exclusively physical observables [57]. Note that an alternative procedure that uses a Helm-type [13,58] weak charge density instead of a SFermi function yields a consistent, yet slightly lower, density than Eq. (11).

How accurately can ρ_0 be measured in the near future? The PREX II campaign has completed data taking with a goal of measuring $R_{\rm wk}$ to 1%. Figure 3 shows an example baryon density for ^{208}Pb assuming a SFermi weak charge density with $R_{\rm wk} = 5.826$ fm (central PREX value [13]) and $a = 0.62$ fm. We have added the charge density as per Eq. (5). The error band in Fig. 3 includes a 1% error in $R_{\rm wk}$ and a 10% error in a added in quadrature. This total error corresponds to ± 0.004 fm^{-3} in ρ^0_b or about a 2.5% error in ρ_0 that is comparable to our assumed 3% error in $f_{\rm ex}$.

There is strong motivation for an additional parity-violating electron scattering experiment to measure the surface thickness a. Both PREX and PREX II were performed at a momentum transfer of $q \approx 0.475$ fm^{-1} and are primarily sensitive to the weak radius. Instead, a new experiment near $q \approx 0.78$ fm^{-1} is sensitive to a [43]. Following Ref. [59] we have calculated the parity-violating asymmetry A_{pv} for elastic electron scattering including Coulomb distortions [31]. We find that the logarithmic derivative of A_{pv} with respect to $\log(a)$ is about 0.53 at $q = 0.78$ fm^{-1}. Therefore a 5% measurement of A_{pv} can constrain a to 10%. We will discuss this possible experiment in more detail in a forthcoming paper.

IV. CONCLUSIONS

In conclusion, the saturation density of nuclear matter ρ_0 is a fundamental nuclear physics property that is diffi-

cult to predict from chiral effective field theory. Because of nuclear saturation, ρ_0 is closely related to the interior density of a heavy nucleus. We emphasize that the average interior baryon density of ^{208}Pb is an experimentally observable quantity that can be determined with parity-violating electron scattering. We used the existing PREX results for the weak radius to obtain a first measurement of the interior baryon density of ^{208}Pb. We then extrapolated this result to infinite nuclear matter and obtained $\rho_0 = 0.150 \pm 0.011$ fm^{-3}. The quoted 7% error has contributions from the PREX error on the weak radius, uncertainty in a theoretical estimate of the surface thickness a, and the error in extrapolating to infinite nuclear matter. These errors can be improved with the upcoming PREX II results and with a new parity violating electron scattering experiment—at a somewhat higher-momentum transfer—to determine the surface thickness of the weak density. This will allow an accurate determination of ρ_0 that is very closely related to the experimentally measured interior baryon density of ^{208}Pb. As a result of the parity-violating measurements, the theoretical assumptions necessary to extract ρ_0 will be both reduced and clarified.

ACKNOWLEDGMENTS

We thank Witek Nazarewicz, Concettina Sfienti, Dick Furnstahl, and Zach Jaffe for helpful discussions. This material is based on work supported by the US Department of Energy Office of Science, Office of Nuclear Physics under Awards DE-FG02-87ER40365 (Indiana University), DE-FG02-92ER40750 (Florida State University), and DE-SC0018083 (NUCLEI SciDAC Collaboration).

[1] C. F. von Weizsacker, Zeitschr. Phys. (in German) **96**, 431 (1935).
[2] W. D. Myers and W. J. Swiatecki, Nucl. Phys. **81**, 1 (1966).
[3] G. Gamow, Proc. R. Soc. Lond. A **126**, 632 (1930).
[4] H. A. Bethe, Annu. Rev. Nucl. Sci. **21**, 93 (1971).
[5] B. D. Day, Phys. Rev. Lett. **47**, 226 (1981).
[6] S. Weinberg, Phys. Let. B **251**, 288 (1990).
[7] H.-W. Hammer, S. Konig, and U. van Kolck, Rev. Mod. Phys. **92**, 025004 (2020).
[8] R. Machleidt and D. R. Entem, Phys. Rep. **503**, 1 (2011).
[9] C. Drischler, K. Hebeler, and A. Schwenk, Phys. Rev. Lett. **122**, 042501 (2019).
[10] D. Lonardoni, I. Tews, S. Gandolfi, and J. Carlson, Phys. Rev. Res. **2**, 022033 (2020).
[11] P.-G. Reinhard, M. Bender, W. Nazarewicz, and T. Vertse, Phys. Rev. C **73**, 014309 (2006).
[12] S. Abrahamyan *et al.*, Phys. Rev. Lett. **108**, 112502 (2012).
[13] C. J. Horowitz *et al.*, Phys. Rev. C **85**, 032501(R) (2012).
[14] M. Thiel, C. Sfienti, J. Piekarewicz, C. J. Horowitz, and M. Vanderhagen, J. Phys. G: Nucl. Part. Phys. **46**, 093003 (2019).
[15] H. De Vries, C. W. De Jager, and C. De Vries, At. Data Nucl. Data Tables **36**, 495 (1987).
[16] M. Bender, P.-H. Heenen, and P.-G. Reinhard, Rev. Mod. Phys. **75**, 121 (2003).
[17] P. Klüpfel, P.-G. Reinhard, T. J. Bürvenich, and J. A. Maruhn, Phys. Rev. C **79**, 034310 (2009).
[18] P. G. Reinhard and W. Nazarewicz, Phys. Rev. C **93**, 051303(R) (2016).
[19] M. B. Tsang *et al.*, Phys. Rev. C **86**, 015803 (2012).
[20] A. Trzcińska, J. Jastrzebski, P. Lubinski, F. J. Hartmann, R. Schmidt, T. von Egidy, and B. Klos, Phys. Rev. Lett. **87**, 082501 (2001).
[21] B. Kłos *et al.*, Phys. Rev. C **76**, 014311 (2007).
[22] J. Zenihiro *et al.*, Phys. Rev. C **82**, 044611 (2010).
[23] L.-W. Chen, C. M. Ko, and B.-An. Li, Phys. Rev. C **72**, 064309 (2005).
[24] E. Friedman, Nucl. Phys. A **896**, 46 (2012).
[25] C. M. Tarbert *et al.*, Phys. Rev. Lett. **112**, 242502 (2014).
[26] D. Akimov, J. B. Albert, P. An, C. Awe, P. S. Barbeau, B. Becker, V. Belov, A. Brown, A. Bolozdynya, B. Cabrera-Palmer *et al.* (COHERENT Collaboration), Science **357**, 1123 (2017).
[27] D. Akimov, J. B. Albert, P. An, C. Awe, P. S. Barbeau, B. Becker, V. Belov, M. A. Blackston, L. Blokland, A. Bolozdynya *et al.* (COHERENT Collaboration), arXiv:2003.10630.
[28] P. S. Amanik and G. C. McLaughlin, J. Phys. G: Nucl. Part. Phys. **36**, 015105 (2009).
[29] K. Patton, J. Engel, G. C. McLaughlin, and N. Schunck, Phys. Rev. C **86**, 024612 (2012).
[30] T. W. Donnelly, J. Dubach, and I. Sick, Nucl. Phys. A **503**, 589 (1989).
[31] C. J. Horowitz, Phys. Rev. C **57**, 3430 (1998).
[32] D. Vretenar, P. Finelli, A. Ventura, G. A. Lalazissis, and P. Ring, Phys. Rev. C **61**, 064307 (2000).
[33] T. Dong, Z. Ren, and Z. Wang, Phys. Rev. C **77**, 064302 (2008).
[34] J. Liu, Z. Ren, C. Xu, and R. Xu, Phys. Rev. C **88**, 054321 (2013).
[35] C. J. Horowitz, Phys. Rev. C **89**, 045503 (2014).
[36] O. Moreno and T. W. Donnelly, Phys. Rev. C **89**, 015501 (2014).
[37] J. Yang, J. A. Hernandez, and J. Piekarewicz, Phys. Rev. C **100**, 054301 (2019).
[38] T. Suzuki, Phys. Rev. C **50**, 2815 (1994).
[39] The PREX-II proposal (unpublished) [http://hallaweb.jlab.org/parity/prex]
[40] The CREX proposal (unpublished) [http://hallaweb.jlab.org/parity/prex]
[41] Z. Lin and C. J. Horowitz, Phys. Rev. C **92**, 014313 (2015).
[42] D. W. Sprung and J. Martorell, J. Phys. A **30**, 6525 (1997).
[43] J. Piekarewicz, A. R. Linero, P. Giuliani, and E. Chicken, Phys. Rev. C **94**, 034316 (2016).
[44] J. Erler, A. Kurylov, and M. J. Ramsey-Musolf, Phys. Rev. D **68**, 016006 (2003).
[45] K. Nakamura *et al.* (Particle Data Group), J. Phys. G **37**, 075021 (2010).
[46] B. G. Todd-Rutel and J. Piekarewicz, Phys. Rev. Lett. **95**, 122501 (2005).
[47] M. Beiner, H. Flocard, Nguyen van Giai, and P. Quentin, Nucl. Phys. A **238**, 29 (1975).
[48] E. Chabanat, P. Bonche, P. Haensel, J. Meyer, and R. Schaeffer, Nuc. Phys. A **635**, 231 (1998).

[49] M. Kortelainen, T. Lesinski, J. More, W. Nazarewicz, J. Sarich, N. Schunck, M. V. Stoitsov, and S. Wild, Phys. Rev. C **82**, 024313 (2010).
[50] M. Kortelainen, J. McDonnell, W. Nazarewicz, P. G. Reinhard, J. Sarich, N. Schunck, M. V. Stoitsov, and S. M. Wild, Phys. Rev. C **85**, 024304 (2012).
[51] F. J. Fattoyev, C. J. Horowitz, J. Piekarewicz, and G. Shen, Phys. Rev. C **82**, 055803 (2010).
[52] G. A. Lalazissis, J. Konig, and P. Ring, Phys. Rev. C **55**, 540 (1997).
[53] W.-C. Chen and J. Piekarewicz, Phys. Lett. B **748**, 284 (2015).
[54] J. Piekarewicz and M. Centelles, Phys. Rev. C **79**, 054311 (2009).
[55] G. Hagen, T. Papenbrock, D. J. Dean, and M. Hjorth-Jensen, Phys. Rev. C **82**, 034330 (2010).
[56] G. Hagen, A. Ekstrom, C. Forssen, G. R. Jansen, W. Nazarewicz, T. Papenbrock, K. A. Wendt, S. Bacca, N. Barnea, B. Carlsson, C. Drischler, K. Hebeler, M. Hjorth-Jensen, M. Miorelli, G. Orlandini, A. Schwenk, and J. Simonis, Nat. Phys. **12**, 186 (2016).
[57] W.-C. Chen and J. Piekarewicz, Phys. Rev. C **90**, 044305 (2014).
[58] R. H. Helm, Phys. Rev. **104**, 1466 (1956).
[59] C. J. Horowitz, S. J. Pollock, P. A. Souder, and R. Michaels, Phys. Rev. C **63**, 025501 (2001).